SUB 1-MILLIMETER SIZE FRESNEL MICRO SPECTROMETER

Yeonjoon Park

National Institute of Aerospace, Hampton, VA, 23681, USA

Laura Koch, Kyo D. Song

Optical Engineering, Dept. of Engineering, Norfolk State University, Norfolk, VA, 23504, USA

SangJoon Park

Chemistry Dept., Kyungwon University, Kyungki-do, 461-701, Korea

Glen King, Sang Choi

NASA Langley Research Center, Hampton, VA, 23681, USA

Abstract

An ultra-small micro spectrometer with less than 1mm diameter was constructed using Fresnel diffraction. The fabricated spectrometer has a diameter of 750 micrometers and a focal length of 2.4 mm at 533nm wavelength. The micro spectrometer was built with a simple negative zone plate that has an opaque center with an ecliptic shadow to remove the zero-order direct beam to the aperture slit. Unlike conventional approaches, the detailed optical calculation indicates that the ideal spectral resolution and resolving power do not depend on the miniaturized size but only on the total number of rings. We calculated 2D and 3D photon distribution around the aperture slit and confirmed that improved micro-spectrometers below 1mm size can be built with Fresnel diffraction. The comparison between mathematical simulation and measured data demonstrates the theoretical resolution, measured performance, misalignment effect, and improvement for the sub-1mm Fresnel micro-spectrometer. We suggest the utilization of an array of micro spectrometers for tunable multi-spectral imaging in the ultra violet range.

I. INTRODUCTION

A tiny spectrometer with a small prism or grating can be utilized for applications such as a hyper spectral microscope[1], spectral measurement of molecular light source in a tiny confined volume such as inside a cryostat[2], miniaturized Raman spectroscopy for *in-vivo* medical research[3], and mini-spectral scanner for multiple optical fibers. Since the miniaturization of a spectrometer has great technological and commercial importance, there have been significant efforts to reduce the size of a spectrometer. For example, Hamamatsu photonics developed 1-inch cube mini-spectrometer with 9nm spectral resolution, I. Avrutsky et al.[4] built a compact 1cm spectrometer, P. Montgomery et al.[5] fabricated a miniature 5mm x 5mm x 0.5mm Fourier transform spectrometer, and N. Kitaura et al.[6] demonstrated a mini-spectrometer having a 4.5mm diameter with 14.83mm focal length based on a whole transparent molded plastic Fresnel lens. While most of the today's spectrometers use the Fraunhofer diffraction equation with a linear grating, the approach with Fresnel diffraction has a fundamental advantage in miniaturization. Although Fraunhofer diffraction[7] is valid when the optical distance Z is large such that $Z >> \boldsymbol{a}^2/\lambda$ where $\boldsymbol{a}$ is the diameter of an aperture and λ is the wavelength of the light, Fresnel diffraction is valid for very small optical distances such that $Z << \boldsymbol{a}^2/\lambda$. Therefore Fresnel diffraction is a better mathematical foundation for the ultimate miniaturization of small Z. Recently, there has been a strong interest for gratings in the deep Fresnel field as well.[8] The early design of N. Kitaura et al.[6] used a whole transparent plastic Fresnel lens with saw-tooth blades for the high light-collection efficiency, which was originally developed for a laser collimator. However, this lens was designed for a specific target wavelength with a limited working spectral range for optimal photon confinement at the focal point. It has zero-order direct beam noise from the center of a lens and it is very difficult to fabricate angled 3D structure in the further miniaturized micro-to-nanometer scales. Also the limit of miniaturization and the size-effect on the spectral resolution were not clear in the previous studies. Therefore, we report an alternate tiny Fresnel spectrometer design with a circular ring grating, having a two-dimensional opaque-centered binary zone plate of 750μm diameter and study the spectral analysis capability and the effect of further miniaturization, i.e. over 200 times smaller optical-path volume compared with previous designs[6]. Unlike the whole transparent Fresnel lens, two-dimensional binary zone plates have lower light collection efficiency (below 50%) but are easier to fabricate on smaller scales and can be used for a wider range of wavelengths because they do not have a specific target wavelength for optimized focusing. Also, our approach can adopt the recent developments of electrically controllable Fresnel zone plates based on liquid crystals[9-11].

II. DESIGN OF FRESNEL MICRO SPECTROMETER

Figure 1 shows the set-up of Fresnel micro-spectrometer with the opaque-center zone plate. The general types of straight-line spectrometers were first proposed with a kinoform lens by P.M. Hirsch et al.[12] in 1970 and demonstrated with a plastic Fresnel lens by N. Kitaura et al.[6] in 1995. A binary zone plate was typically designed with a concentric series of transparent and opaque rings. The radius of each ring is determined by a size coefficient ***K,*** such that $r_n = K\sqrt{n}$ where r_n is the beginning and ending radius of the n_{th} ring and n is the order number. When the transparent rings are built on the annular

zones of n = 0 to 1, 2 to 3, 4 to 5, and so on, a positive zone plate with a transparent center is constructed as shown in the inset picture (a) of Figure 1. If transparent rings are built on the opposite regions such as the annular zones of n = 1 to 2, 3 to 4, 5 to 6, and so on, a negative zone plate with an opaque center is constructed as shown in the inset picture (b) of Figure 1. Both have the same focal points at $\frac{K^2}{\lambda}, \frac{K^2}{3\lambda}, \frac{K^2}{5\lambda}$, and $\frac{K^2}{(2p-1)\lambda}$ where p is a positive integer. The first (longest) focal point is designated as ***F*** and the next ones as ***F/3***, ***F/5***, and ***F/*** $(\boldsymbol{2p-1})$. The difference is that the positive one has in-phase (0°) photons to the zero-order direct beam at the focal point while the negative one has 180° out-of-phase photons with respect to the direct beam at the focal point. It is very interesting to note that when the radius of the zone plate is miniaturized by ***M*** times with a linear miniaturization factor ***M*** such that $r_n = \frac{K}{M}\sqrt{n}$, the focal length becomes $\frac{K^2}{M^2\lambda}$ which is shortened by $\boldsymbol{M^2}$ times. Therefore when the zone plate is miniaturized by 5 times, the overall thickness due to the focal length is shortened by 25 times, thus approaching a thin-film structure.

The spectrometer structure in Figure 1 uses a negative zone plate with an ecliptic shadow from the opaque center to block the zero-order direct beam. In our approach, the dispersive relation of a zone plate, i.e. the inverse dependence of focal length ***F*** on the wavelength λ, ***F*** = $\frac{K^2}{\lambda}$ was utilized as a spectrometer. The inset picture (c) and main diagram of Figure 1 show the cross-section and 3D set-up of the Fresnel micro-spectrometer. When the optical length Z is changed with a linear scanning actuator, the photon intensity at the detector behind the round aperture slit is recorded with Z which corresponds to $\lambda(z) = \frac{K^2}{Z}$.

III. MATHEMATICAL SIMULATION

When a zone plate of radius α is centered at (0,0,0), the electromagnetic field distribution $u(x,y,z)$ at an arbitrary point (x,y,z) is described by the Fresnel diffraction[13] equation-1 with an integral over the zone plate area (ξ,η,0) where *A* is an initial constant for the incoming uniform parallel light, λ is the wavelength of light, and $k = \frac{2\pi}{\lambda}$.

$$u(x,y,z) = \frac{iA}{\lambda z} e^{-ikz} \times \int\int_{\substack{\xi^2+\eta^2 \le a^2 \\ zone\ \ plate}} \exp\left\{\frac{-\mathrm{ik}}{2\mathrm{z}}[(x-\xi)^2 + (y-\eta)^2]\right\} d\xi d\eta$$ --- equation-1.

On the optical axis, equation-1 is simplified to equation-2 by the circular symmetry, where $2m$ is the total number of rings, r_n is the outer radius of n_{th} ring, and σ is a variable for the radial integral.

$$u(0,0,z) = \frac{2\pi i A}{\lambda z} e^{-ikz} \left[\int_{r_1}^{r_2} + \int_{r_3}^{r_4} + \int_{r_5}^{r_6} + \cdots \int_{r_{2m-1}}^{r_{2m}} \right] e^{-(\frac{ik}{2z})\sigma^2} \sigma d\sigma$$ --- equation-2.

The photon intensity is given by $I(x,y,z) = |u(x,y,z)|^2$.

In order to get the photon intensity distribution for a finite number of rings, the above equations have to be solved numerically. Figure 2 shows the optical simulations from the above equations for three

monochromatic lasers at 450nm, 533nm, and 633nm. In the first row, the photon intensity at the actual optical distance is plotted. In the second row, the photon intensity at the converted wavelength according to the above $\lambda(z)$ equation is plotted. In the first column (a), three different negative zone plates with the same size constant ***K***, but different number of rings are compared as shown in picture (a3). Dotted lines are for a total of 60 rings, dashed lines are for 80 rings, and solid lines are for 100 rings. As the number of rings increases, the full diameter increases and the sharpness of the peaks in the wavelength scan (a2) and optical distance scan (a1) are improved. In the second column (b), two different zone plates with the same number of rings (total 100 rings) and different size constants ***K***s, having different full diameters are compared. The bigger one has a 1,000μm diameter (dotted line) and the smaller one has a 750μm diameter (solid line) but both of them have a total of 100 rings as shown in (b3). They have different focal distance and sharpness of the peaks in the actual optical distance scan as shown in (b1). However, once the optical distance is converted to the corresponding wavelength according to the $\lambda(z)$ equation, they have exactly the same spectral peaks as shown in (b2). Therefore, we conclude that there is no size dependence in the spectral resolution of the micro spectrometer as long as they have the same number of rings. This unanticipated result comes from the fact that when ***K*** is large, the actual optical distance is increased by $\boldsymbol{K}^2$ but another $\boldsymbol{K}^2$ term in the conversion equation $\lambda(z)$ cancels the size effect. In column (c), three different zone plates with the same full diameter (750μm) and different number of rings are compared. The size constant ***K*** is adjusted so that they have the same full diameters. They have different focal lengths and sharpness of the peaks in the optical distance graph (c1). The converted wavelength graph (c2) shows that the spectral sharpness of the peaks depends on the total number of rings only. The converted spectral scan graph (c2) is identical to the previous spectral graph (a2). This confirms that the size of the Fresnel micro spectrometer does not affect the spectral resolution under ideal conditions. However, the fabrication error on the small scale may be significant in actual manufacturing.

Figure 3-(a) shows the spectral resolution of two negative zone plates with 100 rings and 50 rings by the Rayleigh criterion in which the secondary peak is located at the first minima of the primary peak. The Rayleigh criterion has different intensity drops at the middle point, depending on the detailed distribution profile. For example, the Rayleigh criterion on the spatial resolution of an optical microscope with Airy distribution from two adjacent apertures has a 26% intensity drop at the midpoint.[13] The Rayleigh criterion on the spectral resolution of a linear grating with Fraunhofer diffraction has a 19% intensity drop at the midpoint.[13] In our calculation, the Rayleigh criterion on the spectral resolution of the Fresnel micro-spectrometer with a negative zone plate has an 11% intensity drop at the midpoint.

Figure 3-(b) shows the spectral resolution and resolving power for 533nm wavelength in terms of the total number of rings. The calculated spectral resolution $\Delta\lambda$ is inversely proportional to the number of rings such that $\Delta\lambda = \frac{1045\ (nm)}{\#\ of\ rings}$ and the resolving power is $\frac{\lambda}{\Delta\lambda} = 0.5 \times \#\ of\ rings$. The full width at half maximum (FWHM) was 9.26nm. With 100 rings, the spectral resolution is $10.45\ nm$ and resolving power is about 50 and these values are independent from the size. In previous work by N. Kitaura et al.[6], the resolving power of a full-transparent Fresnel lens was estimated to be linearly proportional to the

lens size as $\frac{\lambda}{\Delta\lambda} \fallingdotseq \frac{a}{4\lambda(f/\#)}$, where $f/\#$ is the f-number of a lens and $\boldsymbol{a}$ is the radius of lens. This estimation has hindered further miniaturization without loss of spectral resolution. To the contrary, in our approach, $f/\#$ is not a constant upon the miniaturization because $f/\#$ is defined as $\frac{F}{2a}$, and the focal length ***F*** is shortened by $\boldsymbol{M^2}$ times when the radius $\boldsymbol{a}$ is miniaturized by ***M*** times. Therefore, the resolving power of a Fresnel zone plate does not depend on the size, but depends on the total number of rings only. For comparison, the resolving power of a Fraunhofer linear grating is determined not by the size, but by the total number of lines such that $\frac{\lambda}{\Delta\lambda} = nN$ where n is the refractive index and N is the total number of lines.[13]

Figure 3-(c) shows the 2D photon intensity calculation from equation-1 for a general point (x,0,z) on and off the optical axis. This calculation is made with a total of 50 rings having 500μm diameter. Z axis has a wide range from 400μm to 2900μm including the primary focal point ***F***, ***F/3***, and ***F/5*** focal points. X axis is plotted in a zoomed range between +20μm and -20μm in order to show the details around the focal points. Figure 3-(d) shows the 3D interpretation of a 2D simulation in detail. Smaller ranges of X and Z were used to show the fine features around the focal point ***F***. The low intensity "X" shape around the focal point is a weak light-cone that surrounds the focal point and there is an extended ripple on the optical axis. The light-cones from different wavelengths do not enter the aperture slit because they diverge fast. The center ripples from different wavelengths can enter the aperture slit and cause the interference but the center ripples diminish as the number of ring increases.

IV. FABRICATION AND EXPERIMENT SET-UP

Several units of negative zone plates with different diameters and total number of rings were fabricated with e-beam lithography[14] and focused ion beam[15]. Figure 4 shows Scanning Electron Microscope (SEM) image of a fabricated 750μm diameter negative zone plate comprised of 100 rings. The stage was tilted to 52° with respect to the electron gun when this image was taken. The top layer was coated with Au of 400nm thickness on top of a quartz substrate and Ga^+ ion beam was used with an enhanced etching gas, Xenon difluoride (XeF_2)[16,17] to obtain optically flat and smooth surface. Figure 5 shows the experimental set-up for the optical test. Two lasers of 533nm and 633nm were roughly mixed with a beam splitter. A beam chopper was used to block and pass the mixed laser beams at a frequency of 192Hz. The binary modulation signal from the beam chopper was connected to the reference line of a lock-in amplifier. A spatial filter was inserted to get a uniformly mixed TEM_{00} beam from two lasers. The ring grating module with the negative zone plate was connected to a movable XYZ stage with 0.1 μm steps. X and Y stage movements were used for alignment and Z stage movement was used for changing and scanning the optical distance. The aperture slits of 10—25 μm diameters were used in front of a blue-enhanced silicon photon detector. The signal from the photon detector was connected to the lock-in amplifier with the current amplification of 10^6 V/I. The synchronized lock-in amplification of the modulated photon signal removes the noise from room light and other stray lights. An automatic program was built to align XY stages, scan Z-distance, collect the photon intensity, and calculate the spectral distribution.

Figure 6 shows the photo of a mixed beam on the ring grating module after it passed the spatial filter. The size of ring grating made of a negative zone plate is only 0.75mm and the diameter of uniformly mixed beam is about 5mm as shown in Figure 6-(a). The mixed beam appears as bright yellow color to the human eye and digital camera because they have only three color sensors, red, green, and blue. When the mixed beam is separated by a negative zone plate of 40 rings, about 90% of photons are separated according to the focal distance as shown in Figure 6-(b) and Figure 6-(c) which are the digital camera images of passing lights on a screen after the aperture slit. Both of the images have residual photons of different colors from unwanted wavelengths at the center. When the photons of the correct wavelength pass the aperture slit with a large divergence angle, the stray light from different wavelengths passes the aperture with a narrow confinement at the center. We explain these central residual photons as the center ripple effect in the optical simulation Figure 3-(d). The ripples on the optical axis diminish as the number of rings increases.

V. RESULT AND DISCUSSION

A negative zone plate with a total of 100 rings in 750μm diameter and an aperture slit of 10μm diameter were used in the automated spectral data acquisition in Figure 7. The actual scan distance is from 1mm to 7mm to cover the wavelengths from 200nm to 1100nm. Figure 7-(a) shows the graph of measured photon intensity vs. optical length and Figure 7-(b) shows the graph of the photon intensity vs. the wavelength which is converted by $\lambda(z) = \frac{K^2}{Z}$ from the actual optical length. The photon intensity was measured with photocurrent in pico-ampere (pA) unit from unbiased blue-enhanced silicon photodiode. The measured FWHM of 533nm green laser was 20.3nm in Figure 7-(b). This corresponds to $\Delta\lambda = 22.9\text{nm}$ of Rayleigh criterion and the resolving power of 23.2. Since the actual FWHM of a green laser is less than 1nm, the large FWHM comes from the instrumental broadening of a micro spectrometer and it can be improved by increasing the number of rings. Figure 7-(c) shows the spectral scan with a 533nm green laser as shown in the inset picture. Figure 7-(d) shows the spectral scan with a 633nm red laser as shown in the inset picture. Figure 7-(e) shows the spectral scan with a mixed beam of 533nm and 633nm lasers which looks like yellow light in the inset picture. In the inset pictures, a white bar was inserted in the beam path to show the color of the light. Dashed lines are the references for the 533nm and 633nm wavelengths. Most of the photons exist at the focal points that make the strong peaks at the correct converted wavelengths. However, there are small amounts of stray light to the left and right side of major peaks. These small stray peaks are likely to be the zero-order direct beams from adjacent transparent rings when the ring grating module is slightly misaligned with a small tilt angle. Since the optical distance between the two lasers is about 200μm and the aperture diameter is only 10μm, the required angular tolerance to keep half of the aperture slit on the correct optical axis is $\arctan\left(\frac{5}{200}\right)$ =1.4°. Therefore high angular accuracy is required in the optical alignment between the optical axis and scanning axis. The peak at 533nm wavelength peak has a truncated summit while the peak at 633nm has a full summit at the desired point. This is because the optical system was aligned for 633nm focal point so that the accumulated photons with 533nm wavelength fall on a slightly different point next to the aperture when the Z-scan is at the exact optical distance for 533nm wavelength. These

data show that the fabricated Fresnel micro-spectrometer of 0.75 mm size can acquire spectral information as expected but relatively high alignment accuracy for both of X- and Y-direction is required to avoid artifacts. In the Fraunhofer linear grating, the alignment on the Y-direction which is parallel to the line grooves can be loose because the linear slit accepts the broad width of lights in the Y-direction. Another source of error is that the focused ion beam machine had about 3% tolerance in the X/Y aspect ratio. 3% of the full radius of 375μm is 11μm which can be larger than the width of outer rings. Therefore the inaccuracy of the X/Y aspect ratio may result in a large FWHM due to imperfect confinement of photons at the focal point as well.

Figure 8 shows an array of negative zone plates with 1mm x 1mm pitch. If this array is combined with individual aperture slit and detector, the small size and pitch allow a dense integration of 100 x 100 = 10,000 micro-spectrometers in a 10cm x 10cm area. The spectral resolution of 23nm is similar to the bandwidth of common optical filters which are used for multi-spectral CCD imaging. Therefore, we suggest that an array of micro-spectrometers can afford tunable multi-spectral imaging. Such a system can remove the necessity to exchange numerous filters to get multiple images with high spectral resolution. When the transparent substrate is made with UV transparent materials such as calcium fluoride (CaF_2)[18], it can operate in the UV range where most liquid crystal based tunable filters[19,20] cannot be used due to UV absorption. Because of sensitivity and requirements for alignment accuracy, it would be necessary to control the XYZ position of aperture slits and detectors individually rather than simultaneously in a group mode.

VI. CONCLUSION

We demonstrated that the spectral resolution and resolving power of an ideal Fresnel micro spectrometer do not depend on the miniaturized size but on the total number of rings only. This is analogous to the spectral relationship of a linear grating with Fraunhofer diffraction. The full 2D/3D simulation of the photon distribution around the focal point reveals weak light cones and central ripples. The fabricated micro spectrometer of 100 rings in 750μm full diameter had a spectral resolution of 22.9nm and resolving power of 23.2. These values are about half of the best theoretical resolving power due to small misalignment and inaccurate manufacturing. The volume of the optical path in the fabricated micro spectrometer is $\pi \cdot \left(\frac{0.75(mm)}{2}\right)^2 \cdot 2.4(mm) = 1.06\ mm^3$ for 533nm light. This is about 230 times smaller than the volume obtained by previous spectrometers[6]. We conclude that further miniaturized and improved spectrometers based on Fresnel diffraction can be built if the total number of rings is kept constant or increased and the fabrication accuracy is improved.

VII. ACKNOWLEDGEMENT

The authors appreciate the assistance of Ms. Pokeun Han and Ms. Seojin Kim with the focused ion beam machine. This research was supported by the space act agreement SAA-15546 of NASA, USA and KOSEF program by the ministry of science and technology, Republic of Korea.

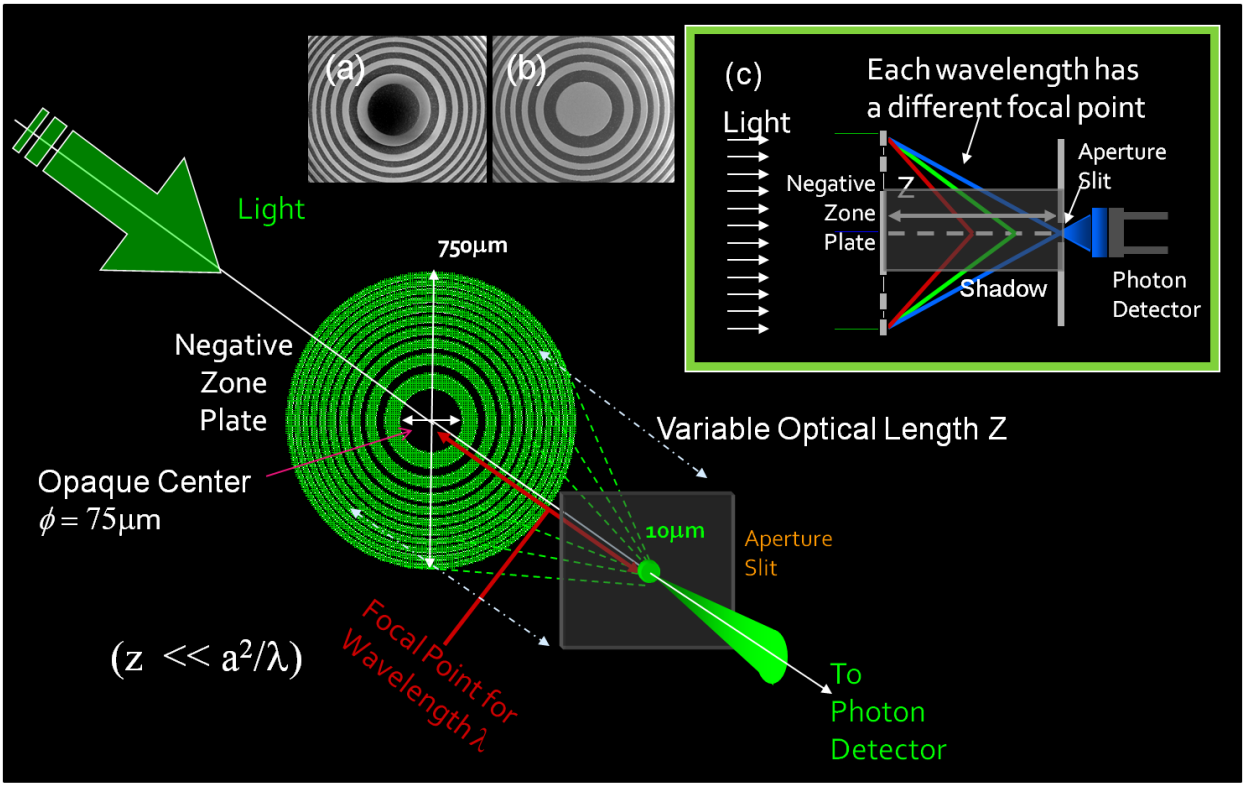

Figure 1. Optical set-up diagram of Fresnel micro spectrometer with negative zone plate, Inset pictures: (a) positive zone plate with a transparent center, (b) negative zone plate with an opaque center, (c) cross-sectional view

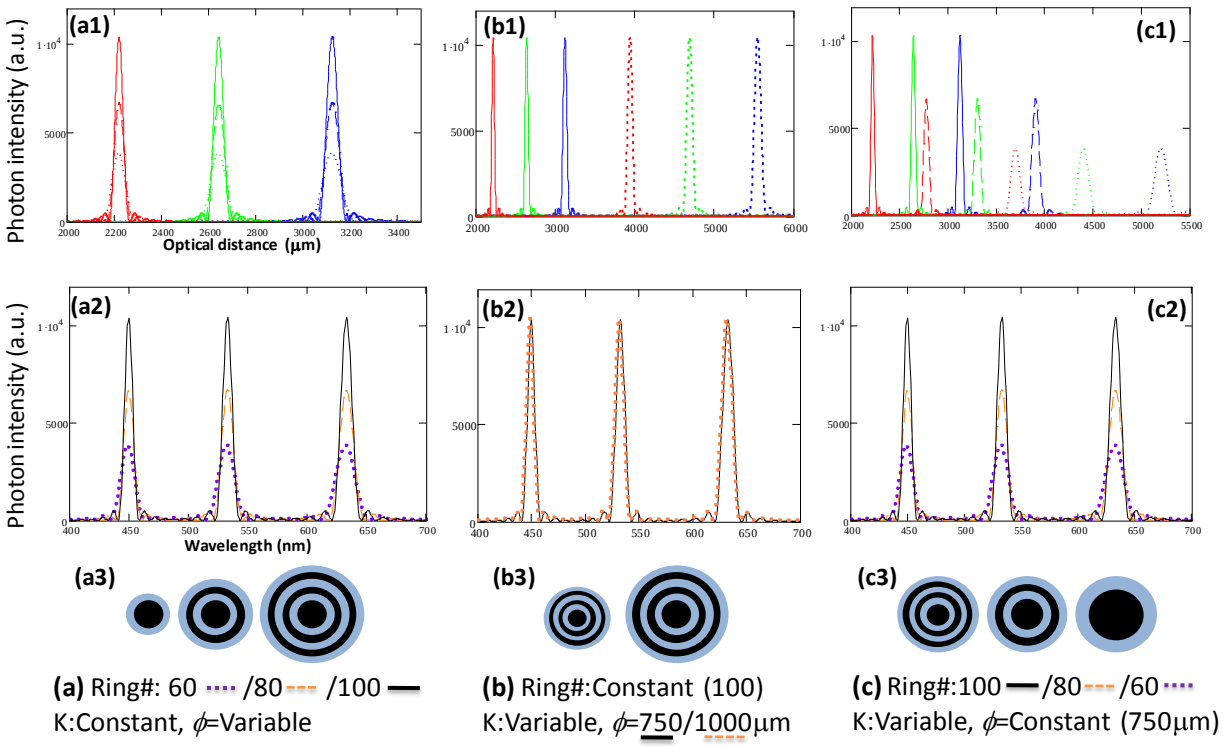

Figure 2. Optical simulation of normalized photon intensity vs. (1) optical distance and (2) scanned wavelength in different ring gratings; (a) constant K, variable number of rings, (b) constant number of rings, variable outer diameter(ϕ), (c) same outer diameter, but different number of rings. Inset pictures (a3), (b3), and (c3) show the comparison schemes.

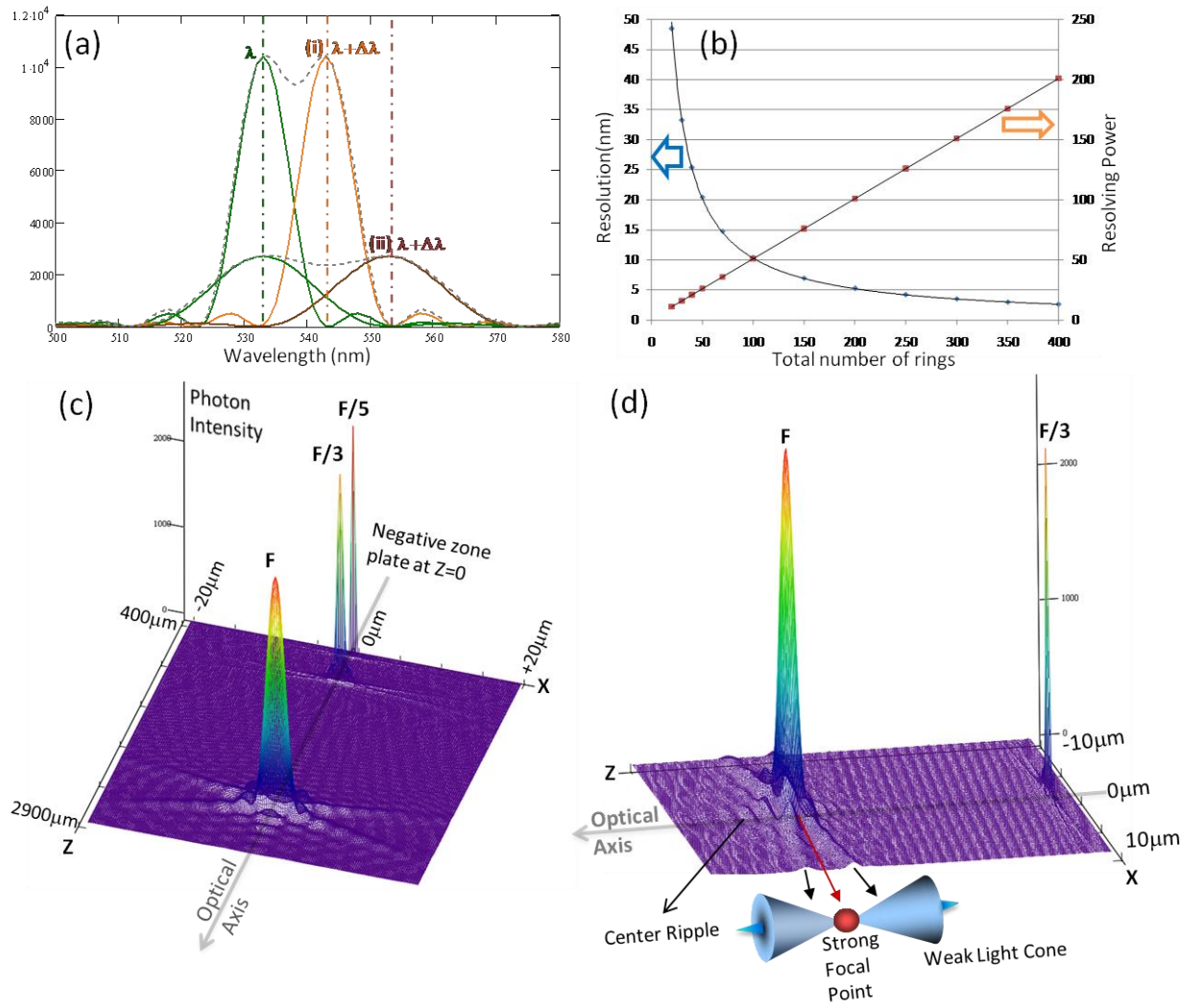

Figure 3. (a) Spectral resolution by Rayleigh criterion (i) total 100 rings, (ii) total 50 rings, (b) Spectral resolution and resolving power vs. total number of rings, (c) Photon intensity simulation around focal points in a general 2D plane, (x,0,z) - on and off the optical axis, (d) 3D interpretation of 2D photon intensity simulation

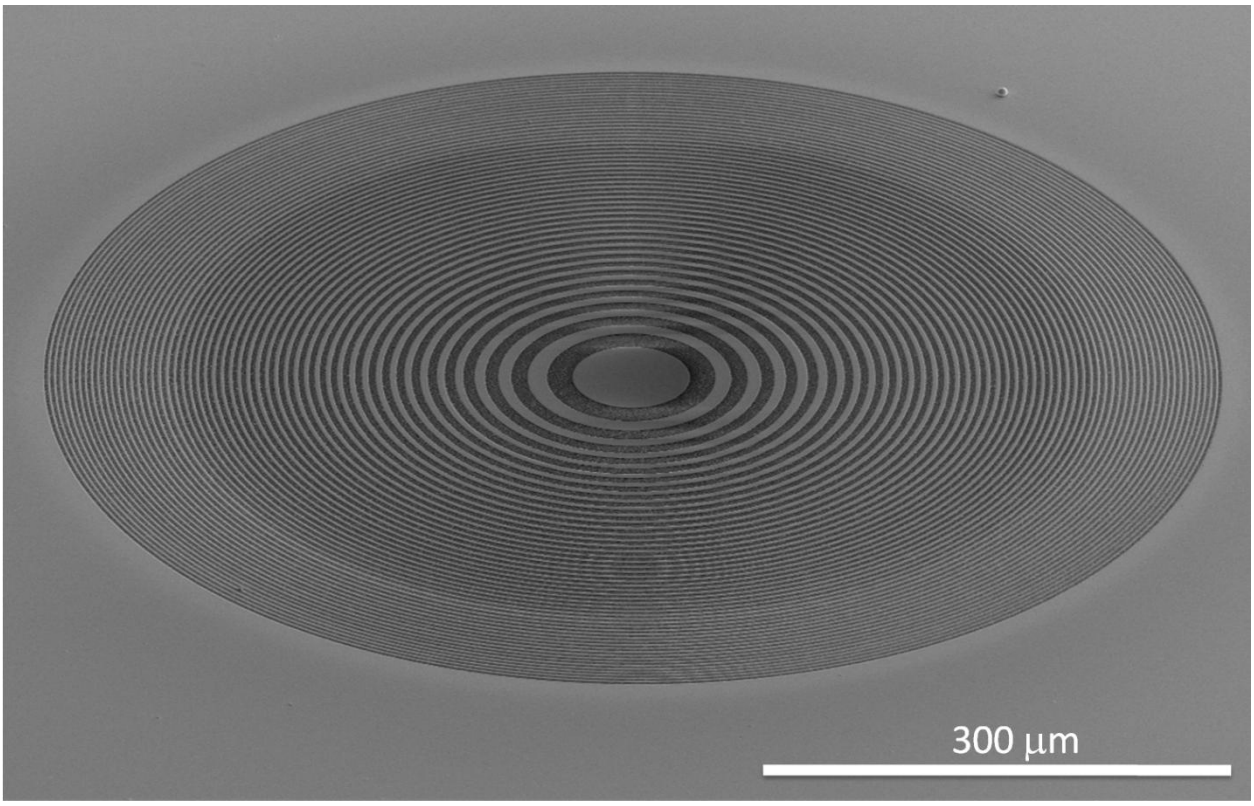

Figure 4. SEM image of fabricated negative zone plate with 100 rings (50 transparent and 50 opaque rings), stage tilt = 52°

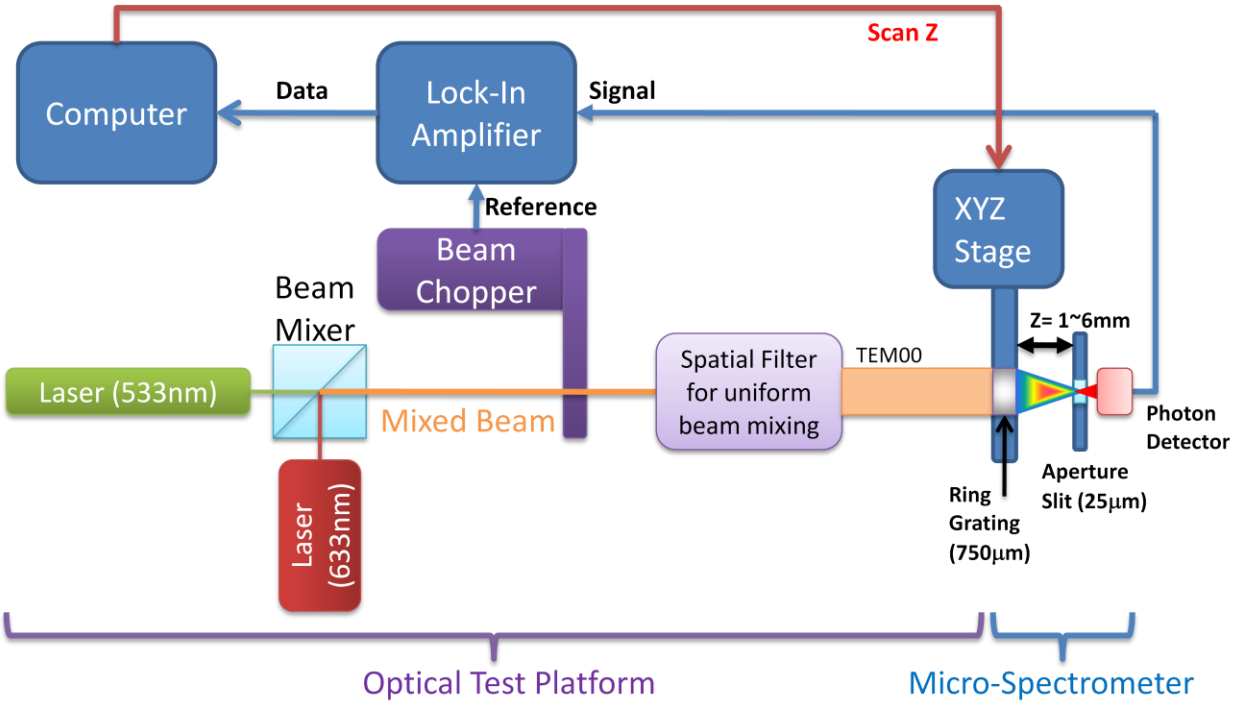

Figure 5. Optical test set-up diagram

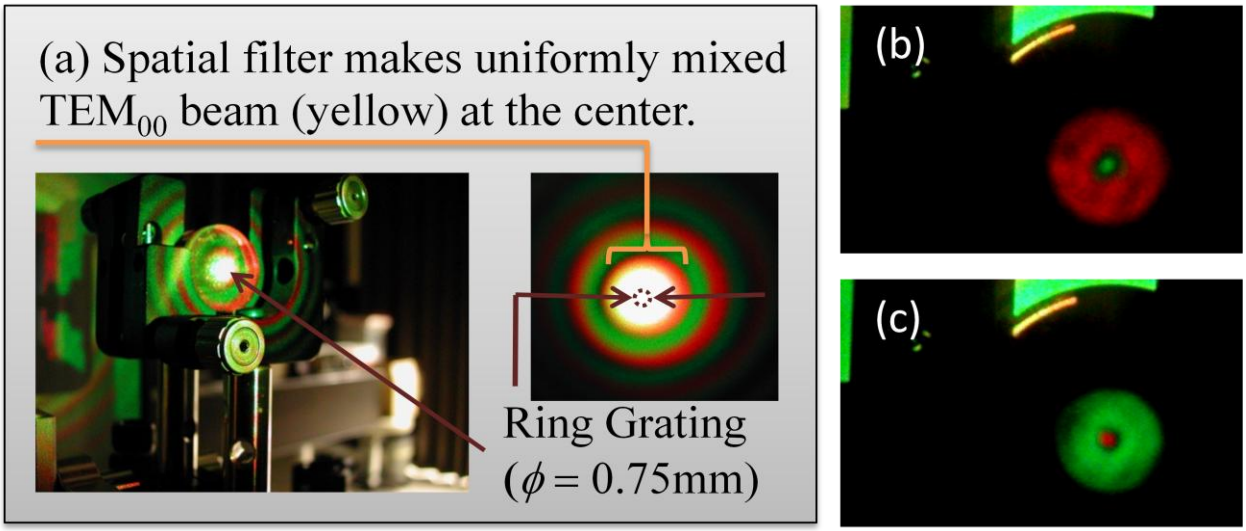

Figure 6. (a) Uniformly mixed beam (yellow color) falls on the ring grating, (b) transmitted light through the aperture slit at the red focal point, (c) at the green focal point.

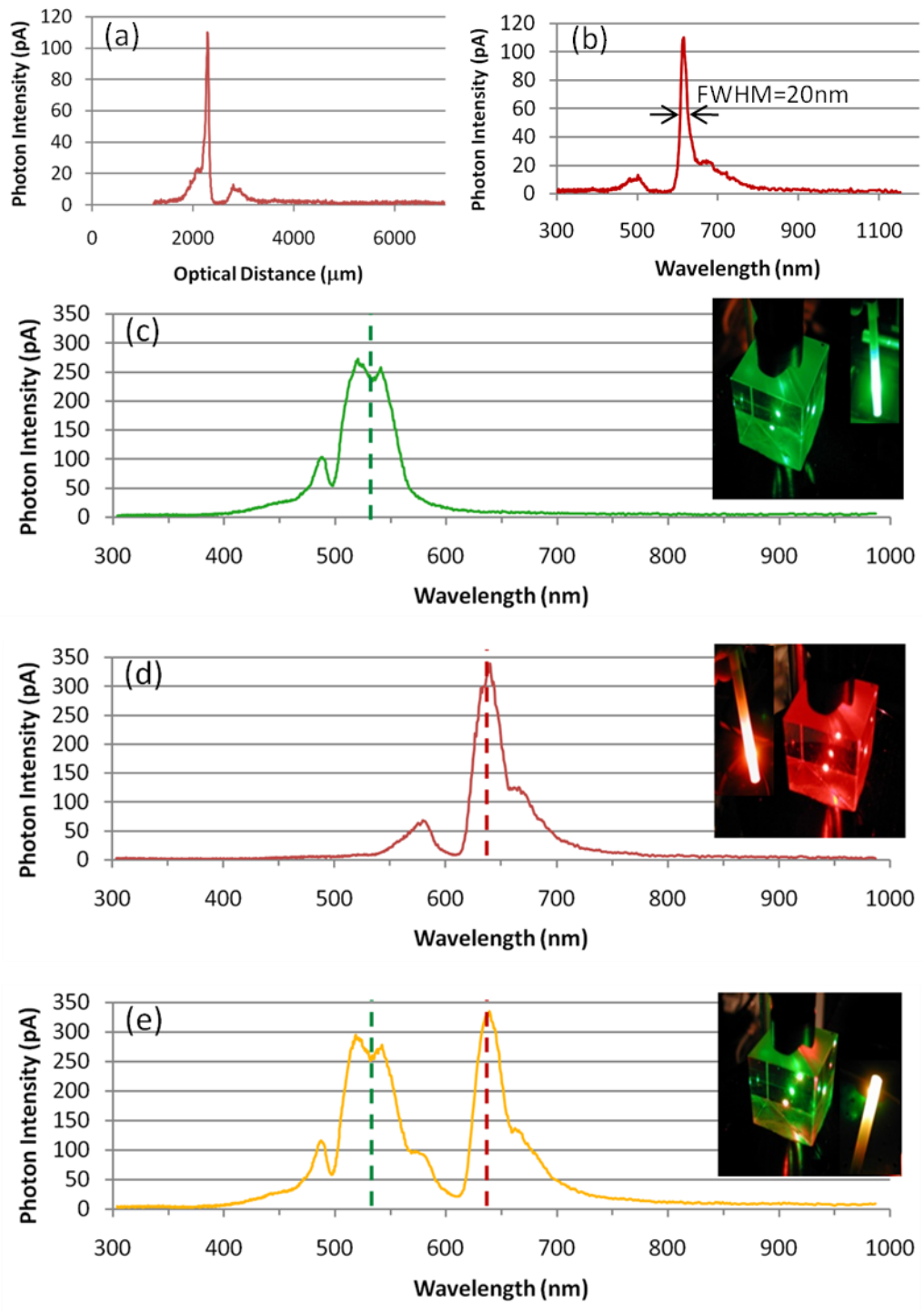

Figure 7. Measured data, (a) intensity vs. optical distance, (b) intensity vs. wavelength, (c) spectral data with 533nm laser, (d) spectral data with 633nm laser, (e) spectral data with mixed beam, 533nm and 633nm lasers.

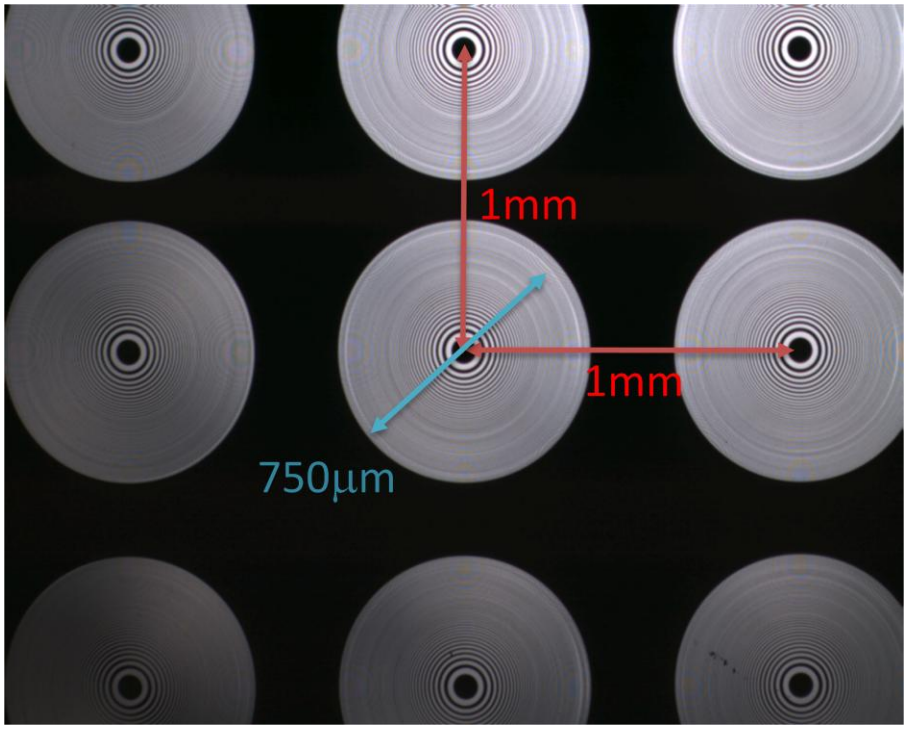

Figure 8. Array of Fresnel micro-spectrometers

Reference

[1] M. B. Sinclair, D. M. Haaland, J. A. Timlin, and H. D. T. Jones, Applied Optics **45,** 6283-6291 (2006).

[2] Y. Khang, Y. Park, M. Salmeron, and E. R. Weber, Review of Scientific Instruments **70,** 4595-4599 (1999).

[3] E. B. Hanlon, R. Manoharan, T. W. Koo, K. E. Shafer, J. T. Motz, M. Fitzmaurice, J. R. Kramer, I. Itzkan, R. R. Dasari, and M. S. Feld, Physics in Medicine and Biology **45,** R1-R59 (2000).

[4] I. Avrutsky, K. Chaganti, I. Salakhutdinov, and G. Auner, Applied Optics **45,** 7811-7817 (2006).

[5] P. C. Montgomery, D. Montaner, O. Manzardo, M. Flury, and H. P. Herzig, Thin Solid Films **450,** 79-83 (2004).

[6] N. Kitaura, S. Ogata, and Y. Mori, Optical Engineering **34,** 584-588 (1995).

[7] Y. Park, J. D. Wright, J. D. L. Jensen, G. C. King, and S. H. Choi, Measurement Science & Technology **16,** 2208-2212 (2005).

[8] S. Teng, N. Zhang, Q. Dong, and C. Cheng, Journal of the Optical Society of America a-Optics Image Science and Vision **24,** 3636-3543 (2007).

[9] Y. H. Fan, H. W. Ren, and S. T. Wu, Optics Express **11,** 3080-3086 (2003).

[10] M. Honma and T. Nose, Japanese Journal of Applied Physics Part 1-Regular Papers Short Notes & Review Papers **44,** 287-290 (2005).

[11] T. H. Lin, Y. H. Huang, A. Y. G. Fuh, and S. T. Wu, Optics Express **14,** 2359-2364 (2006).

[12] P. M. Hirsch, J. A. Jordan, and L. B. Lesem, IBM Technical Disclosure Bulletin **12,** 1806 (1970).

[13] A. Ghatak and K. Thyagarajan, *Optical Electronics* (Cambridge University Press, New York, 1989).

[14] T. Fujita, H. Nishihara, and J. Koyama, Optics Letters **6,** 613-615 (1981).

[15] M. Yasumoto, S. Tamura, N. Kamijo, Y. Suzuki, M. Awaji, A. Takeuchi, H. Takano, Y. Kohmura, and K. Handa, Japanese Journal of Applied Physics Part 1-Regular Papers Short Notes & Review Papers **40,** 4747-4748 (2001).

[16] J. D. Casey, A. F. Doyle, R. G. Lee, D. K. Stewart, and H. Zimmermann, Microelectronic Engineering **24,** 43-50 (1994).

[17] J. Taniguchi, N. Ohno, S. Takeda, I. Miyamoto, and M. Komuro, Journal of Vacuum Science & Technology B **16,** 2506-2510 (1998).

[18] G. Kopitkovas, T. Lippert, C. David, A. Wokaun, and J. Gobrecht, Thin Solid Films **453-54,** 31-35 (2004).

[19] Y. Saito, T. Matsubara, T. Koga, F. Kobayashi, T. D. Kawahara, and A. Nomura, Review of Scientific Instruments **76,** 106103 (2005).

[20] J. Y. Hardeberg, F. Schmitt, and H. Brettel, Optical Engineering **41,** 2532-2548 (2002).